Pulse Radiolysis Study of Solvated Electron Pairing with Alkaline Earth Metals in Tetrahydrofuran. 3. Splitting of p-Like Excited States of Solvated Electron Perturbed by Metal Cations

F. Renou, P. Archirel, P. Pernot, B. Lévy, and M. Mostafavi*

Laboratoire de Chimie Physique, CNRS UMR 8000, Université Paris-Sud, Centre d'Orsay, Bât. 349, 91405 Orsay Cedex, France

Received: July 2, 2003; In Final Form: October 30, 2003

The formation and decay rate constants of the pairs (M^{II}, e^-_s) involving solvated electron and alkaline earth metal cations ($M^{II} = Sr^{II}$, Ca^{II}) are determined by pulse radiolysis measurements in tetrahydrofuran (THF). The pairs present a strong reducing character and can reduce biphenyl to biphenylide radical anion. The observed absorption spectra of the pairs are broad and intense, similar to that of (Mg^{II}, e^-_s). Compared to the absorption spectrum of solvated electron which is a single band located around 2250 nm, these absorption spectra are shifted to the blue and present two bands. The structure of the pairs is investigated by ab initio calculations, and their absorption bands are studied with an asymptotical method. The observation of two absorption bands for the pairs (M^{II}, e_s^-) is rationalized as a perturbation of the solvated electron by neighboring solutes which stabilize differently its s and p states and split the p states. The absorption spectra are compared with those obtained for the pair of solvated electron and alkali metal cations.

I. Introduction

The solvated electron can be formed in a variety of solvents and has been intensively studied during the past decades. First results on the optical absorption of solvated electron were obtained in water in 1962.[1] Since the 1970s the absorption spectrum of the solvated electron was measured in different solvents such as amines, ethers, and alcohols.[2] The solvated electron in water has attracted special interest due to the importance of water in physics, chemistry, and biochemistry. During the past decade important work was done by several groups to determine the structure of the hydrated electron in its ground and excited states. In neat water, several transient pump−probe spectroscopy studies in the visible/infrared spectral range using femtosecond pulses have been reported.[3] These studies, together with theoretical calculations, showed the existence of several excited states for the hydrated electron.[4] Considering the ground state as an s-like state, evidence is reported for the existence of quasi-degenerated p-like states in water, where the p levels are found by calculations to be separated by approximately 0.5 eV.[5] But only one broad absorption band is always observed in different solvents, and distinct transition from the s-like state to different p-like states has never been reported.

A wealth of information on the reduction of metal ions in aqueous solution has been also obtained in the past 30 years, mostly from pulse radiolysis studies.[6] But in comparison, less work has been done in nonaqueous solutions concerning the reactivity of the solvated electron toward metal cations. Recently, we reported a reaction between solvated electron and Mg^{II} in ethers.[7,8] The rate constant of this reaction was estimated around 6.2×10^9 L mol^{-1} s^{-1} in diethyl ether and tetrahydrofuran (THF).[8] The reaction in diethyl ether and tetrahydrofuran leads to the formation of solvated electron−ion pairs (Mg^{II}, e^-_s).[7,8] As we observed, the rate constant of pairing with magnesium ions is 2 orders of magnitude below the diffusion limit, revealing the presence of a kinetic barrier to the formation of the ion pair: THF being a low dielectric medium, the magnesium ions are in strong interaction with the perchlorate ions and this interaction does not favor the pairing with solvated electron. Theoretical calculations have already shown that solvated electron pairing with Mg^{II} is spontaneous, that it induces a strong rearrangement of the perchlorates, and that it can provoke the departure of one THF molecule from the first coordination shell of Mg^{II}.[8]

In the present study we use nanosecond pulse radiolysis technique to observe the reaction between the solvated electron and two other alkaline earth metal cations (Ca^{II} and Sr^{II}) in THF. The rate constants of the pair formation in the case of Ca^{II} and Sr^{II} are determined and ab initio calculations are used to determine the structure of the pairs. We also show that the absorption spectrum of solvated electron in THF is dramatically affected by the presence of charged metal ions Ca^{II} or Sr^{II}. According to the present results and the previous ones with Mg^{II}, we discuss the effect of the presence of metal cations on the absorption spectrum and on the reactivity of the solvated electron. In particular we focus on the degeneracy and the symmetry of the excited state of solvated electron in THF. The observed spectra are compared to those obtained for the pairs formed with alkaline cations in THF. We use ab initio calculations to estimate the free enthalpy of the pair formation and an asymptotic model for the interpretation of the absorption spectra.

II. Experimental and Theoretical Methods

II.1. Experimental Procedure. Tetrahydrofuran of 99.5% purity was purchased from Fluka and was distilled in the presence of metallic sodium under argon atmosphere to remove water and oxidizing agents. Ultrapure deionized water was used

* Corresponding author. E-mail: mehran.mostafavi@lcp.u-psud.fr.

10.1021/jp035899w CCC: $27.50
Published on Web 01/20/2004

to prepare the aqueous solutions. The alkaline earth perchlorates, purchased from Aldrich, were used as received.

A Radiometer Copenhagen CDM 210 was used for the conductivity measurements. The measurements range was from 0.01 to 5.99 μS cm^{-1}, with different frequencies defined for the specific conductivity domain. The cell constant is calibrated before each experiment with solutions of KCl, and the value is around 0.88 cm^{-1}. The two electrodes are made with platinum and do not react with THF. All the conductance measurements are done at room temperature. The conductivity of the pure solvent is below the detection threshold.

The pulse radiolysis setup has been described elsewhere.[9] Electron pulses (3 ns duration) were delivered by a Febetron 706 accelerator (600 keV electron energy) to samples contained in a quartz suprasil cell through a thin entrance window (0.2 mm) having an optical path length (1 cm) perpendicular to the electron beam. The cell was deaerated by a nitrogen flow before the experiment. The solution was changed after each pulse. The optical absorption of the transient species was recorded by means of a classical xenon lamp, monochromator, and photomultiplier or diode setup with a sensitive surface of 1 mm radius. The spectrophotometric detection system had an overall rise time of 3.7 ns in the visible spectral domain and 12 ns in the infrared one.

II.2. Data Analysis of Transient Signals. Transient absorbance signals $A(t,\lambda)$ are expressed as

$$A(t,\lambda) = \sum_{i=1}^{N} c_i(t;\mathbf{K})\epsilon_i(\lambda) \qquad (1)$$

where t is the time, λ is the spectral coordinate, ϵ_i is the extinction coefficient of species i, c_i is the instantaneous concentration, and **K** represents the set of parameters involved in the kinetics model. The concentrations of transient species (c_i) are obtained by numerical simulation of the rate equations corresponding to a set of chemical reactions. Initial conditions are specified through the "initial" concentrations (i.e. just after the pulse) of the precursor species (solvated electron, radicals, etc.). The coupled nonlinear ordinary differential equations are integrated with the LSODA routine, which adapts automatically to stiff or nonstiff conditions.[10] The identification of the parameters is known to be problematic,[11,12] and it is expected that some parameters could not be identified.[13] This state can be improved to some extent with a global analysis strategy, i.e., simultaneous analysis of complementary experiments,[14] and we systematically use that approach in the present work.

We address the identifiability issue with a *practical* identification method based on probabilistic (Bayesian) data analysis.[15,16] It is based on the stochastic sampling by Markov chains[17,18] of the posterior probability density function of the parameters conditional to the observed data, $p(\mathbf{u}|\mathbf{D})$. This method does not focus only on the best fit solution but also on the set of parameters giving an acceptable fit, considering the uncertainty on the analyzed data. Details of the method are given in our previous papers.[8,19]

II.3. Ab Initio Calculations. The neutral solutes, $M(ClO_4)_2$ ($M = Mg^{II}$, Ca^{II}, Sr^{II}) in solution in THF, are investigated with the help of self-consistent field (SCF) and density functional theory (DFT) methods. In the first article of this series we presented results obtained with simplified ab initio calculations.[8] We now give results obtained with more sophisticated methods:

(1) Solvent effect is taken into account with the help of the CPCM cavity model.[20] UAHF radii[20] are used for metals and THF molecules. An unique spherical cavity, centered on Cl, is used for perchlorates. The radius of this sphere (3.0 Å) reproduces the UAHF result for isolated ClO_4^- in THF. For anions we have added a spherical cavity (radius: 2.5 Å), centered at 1 Å away from the metal. This additional cavity prevents the electron from penetrating the dielectric medium.

(2) We have used a 6-31g* basis set for THF, perchlorates, Mg, and Ca, and the SDD basis set and core pseudopotential for Sr. For anions we have added diffuse Gaussians on the metals: for Mg two s and two p (exponents: 0.02, 0.01), for Ca and Sr three s and three p (exponents: 0.01, 0.005, 0.002) and three d (exponents: 0.1, 0.03, 0.01). For the three anions additional s Gaussians (exponents: 0.4, 0.2, 0.1, 0.05) have been centered at 1.0 Å away from the metal, and eventually four p Gaussians with the same exponents, for the excited-states calculations.

(3) Geometries of neutral perchlorates and of their anions have been optimized at the SCF level, and then a single point calculation at the DFT/B3LYP level has been performed.

(4) As mentioned in the previous paper,[8] the number of THF molecules in the first solvation shell is not known and can be two, three, or four according to the mono- and bidentate ligandation of perchlorates. We have not investigated the structure of the first solvation shell and decided to work with two explicit THF molecules only. This means that, in the neutral solute, both perchlorates are bidentate. This number is determined by the present choice of methods, yielding difficult cavity building and long geometry optimizations. We shall see that for Mg we get thermochemical results in good agreement with measurements.

(5) Absorption spectra of the anions have been calculated with the help of the time-dependent DFT (TD/DFT) method.

All the calculations have been carried out using the Gaussian 98 program package.[20]

II.4. Asymptotic Method for the Absorption Spectra Determination. Although the precise nature of the solvated electron is still in debate,[21] the simple image of an electron trapped in a solvent cavity proves very useful. This image is confirmed by molecular dynamics simulations of an electron in water.[5] We thus describe the solvated electron in THF as a single electron problem:

(1) The Hamiltonian contains a kinetic term and no explicit potential term.

(2) The ground and first excited states of the electron are described by a triplet of s, p, and d Gaussian functions, with the same exponent α. The cavity is thus simulated by the spatial extension of the s Gaussian.

(3) The exponent α is adjusted, so as to yield a value of the s $\rightarrow$ p transition energy equal to the experimental value in THF (0.59 eV). Since the kinetic energies of an electron in a s and in a p Gaussian orbital of exponent α amount to 3/2 α and 5/2 α, respectively, we find that the exponent of the Gaussians must be equal to the transition energy: $\alpha = 0.0413$ Å^{-1}. This value is consistent with the cavity radius in THF: 3.4 Å.

With this model the perturbation of the solvated electron by various solutes can be easily studied. Solutes are modeled in the following way:

(1) Alkali cations are modeled with a simple point charge.

(2) Complex solutes are modeled with the help of their Merz−Kollman (MK) charges.[20] MK charges are atomic charges, adjusted so as to reproduce the ab initio values of the electrostatic potential in the space around the solute.

We have calculated in this way potential energy curves for alkali cations and alkaline earth perchlorates in interaction with the solvated electron. Actually, realistic potential curves should be a function of the scaled distance ϵR, taking the environment into account. Since the value of the dielectric constant ϵ of THF is not well-defined for middle-range distances, and since the R parameter will be considered adjustable, we will use the "vacuum" distance R. This method presents a few shortcomings. First, the solute−electron distance is a free parameter, to be adjusted. Second, since solutes are described with point charges and no basis set, the values of oscillator strengths calculated with $\vec{r}$ and $\vec{p}$ integrals generally do not coincide. This means that oscillator strengths are not very reliable. Last, the core repulsion of the solutes is not taken into account. Nevertheless, we shall see that this method is very fruitful.

III. Results and Discussion

III.1. Conductivity Measurements. As for magnesium perchlorate, there is a lack of information about the nature of calcium and strontium perchlorates in THF. We performed therefore conductivity measurements for these two salts. The setup was previously described, and its application range, between 0.01 μS cm^{-1} and 5.99 S cm^{-1}, means that we cannot determine the conductivity of pure THF or very dilute solutions because in these cases the value is below the threshold of the apparatus. In this paper, the concentrations of salts were taken from 6×10^{-4} to 1×10^{-2} mol dm^{-3}, and the corresponding specific conductivities were higher than 0.09 μS cm^{-1}.

Calcium perchlorate is tetrahydrated, and strontium perchlorate is hydrated but we have no indications about the exact number of water molecules for each strontium salt molecule. In the absence of the salts, we added an equivalent amount of water to THF and we observed that the variation of the conductivity is too small to be measured. Therefore, in the presence of the salts, for conductivity measurements, the small quantity of water does not interfere with results because of the slight dissociation of water molecules.

Figure 1 shows the specific conductivity of calcium and strontium salts measured in THF. Experimental data could not be fitted by the Onsager law, and as equilibrium 2 is similar to that of a monovalent system, because we take into account only the dissociation of one perchlorate, we can use the Fuoss−Kraus theory of the triple ion. This method has also been applied for the study of the dissociation of sodium perchlorate in THF. According to the Fuoss and Kraus theory of the triple ion described elsewhere,[22] we assume the reactions of dissociation

$$M^{II}ClO_4^{+} + ClO_4^{-} \rightleftharpoons M^{II}(ClO_4)_2 \qquad K_2 \qquad (2)$$

$$M^{II}(ClO_4)_2 + ClO_4^{-} \rightleftarrows M^{II}(ClO_4)_3^{-} \qquad K_3 = K_T \qquad (3)$$

$$M^{II}(ClO_4)_2 + M^{II}ClO_4^{+} \rightleftarrows M_2^{II}(ClO_4)_3^{+} \qquad K_4 = K_T \qquad (4)$$

where M^{II} is Ca^{II} or Sr^{II}. The notion of triple ion provided by Fuoss−Kraus indicates that there is a possibility of association between three species: one dissociated ion ($MClO_4^+$ or ClO_4^-) and neutral form $Mg(ClO_4)_2$. Consequently, the "triple ion" is either $Mg(ClO_4)_3^-$ or $Mg_2(ClO_4)_3^+$. It means that the total dissociation leading to M^{2+} and two ClO_4^- is completely neglected in our case. Without information on K_3 and K_4, Fuoss and Kraus do the approximation that the two equilibrium constants have similar values, which they justify by considering an average ion size. With these assumptions, we can fit the conductometric results with the relation:

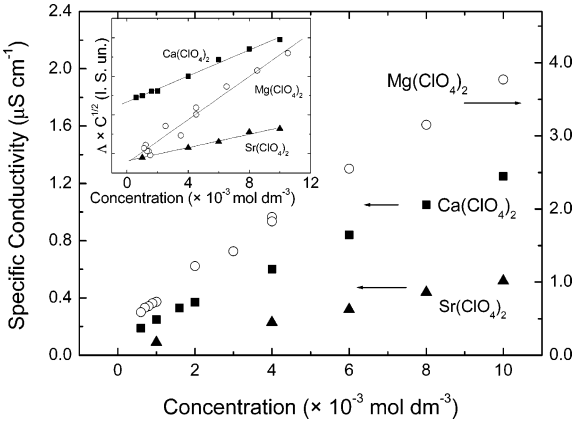

Figure 1. Specific conductivity of $Sr(ClO_4)_2$, $Ca(ClO_4)_2$, and $Mg(ClO_4)_2$ in THF. Inset: Fitting $\Lambda C^{1/2} = f(C)$ according to Fuoss−Kraus theory.

$$\Lambda\sqrt{C} = \frac{\Lambda_0}{\sqrt{K_2}} + \frac{\Lambda^0_T K_T}{\sqrt{K_2}} C \qquad (5)$$

where $K_2 = [M^{II}(ClO_4)_2]/[M^{II}ClO_4^+][ClO_4^-]$ is the association constant for reaction, K_T is the association constant for reactions 3 and 4, assuming the value of K_T is the same for these two reactions. Λ_0 and Λ^0_T are respectively the limiting conductance of the ionic couple of reaction 3 and reaction 4 involving the triple ions. In their theory, Fuoss and Kraus do the approximation that the two equilibrium constants for the formation of triple ions are the same. They explain this approximation by the average ion size computed for the reaction.

In our work, we have to take these ionic associations into account to obtain a good fit of experimental data but the values of the constants K_3 and K_4 have no great importance because we showed that the neutral form is the main species in solution and it reacts with the solvated electrons.

The inset of Figure 1 represents the linear fit of experimental points with the function $\Lambda\sqrt{C} = f(C)$.

For $Ca(ClO_4)_2$ solutions, the intercept of linear fit is 2.3×10^{-5} S cm$^{1/2}$ mol$^{-1/2}$ and the slope is 1.7×10^{-6} S cm$^{7/2}$ mol$^{-3/2}$ with a correlation coefficient of 0.996. To obtain the values of K_2 and K_T, we have to estimate the limiting conductance Λ_0 assuming that Λ^0_T is one-third of Λ_0. Because there are no indications of these values in the literature, we assumed that the variations of Λ_0 between $Mg(ClO_4)_2$ and $Ca(ClO_4)_2$ and then $Sr(ClO_4)_2$ are the same as the one between $Mg(B\varphi_4)_2$, $Ca(B\varphi_4)_2$, and $Sr(B\varphi_4)_2$ ($B\varphi_4$ stands for tetraphenylboron) estimated by De Groof and co-workers.[23]

The limiting conductance of $Ca(ClO_4)_2$ is estimated, for that reason, around 165 S cm^2 mol^{-1}, and in that way we find $K_2 = 5.1 \times 10^8$ mol^{-1} dm^3 ($K_{diss} = 1/K_2 = 2 \times 10^{-9}$ mol dm^{-3}) for reaction 2 and $K_T = 221$ mol^{-1} dm^3 for reactions 3 and 4. It appears that the dissociation in THF is even weaker for calcium perchlorate than for magnesium perchlorate ($K_2 = 7.7 \times 10^7$ mol^{-1} dm^3).[8]

For the $Sr(ClO_4)_2$ solutions, the fit gives an intercept of 8.1×10^{-6} S cm$^{1/2}$ mol$^{-1/2}$ and a slope of 8.6×10^{-7} S cm$^{7/2}$ mol$^{-3/2}$. Assuming the value of 160 S cm^2 mol^{-1} for the limiting conductance of the reaction, we obtain an association constant of 3.9×10^9 mol^{-1} dm^3 for this reaction and 320 mol^{-1} dm^3 for the triple-ion equilibriums. The strontium perchlorate seems to be less dissociated than the two other perchlorate salts in THF.

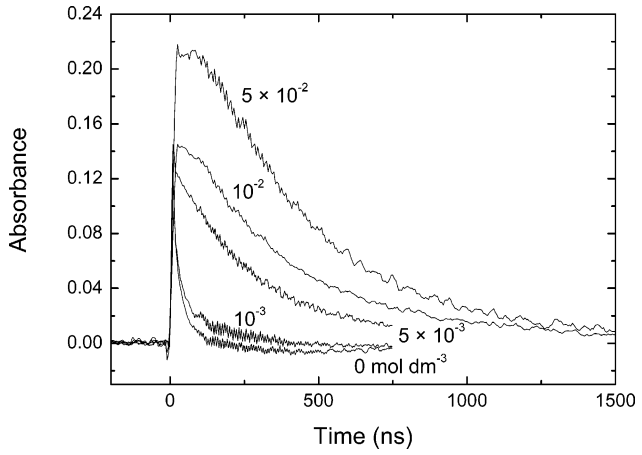

Figure 2. Absorption transient signals at 1000 nm in THF obtained by nanosecond electron pulse for pure solvent, and $Ca(ClO_4)_2$ at different concentration.

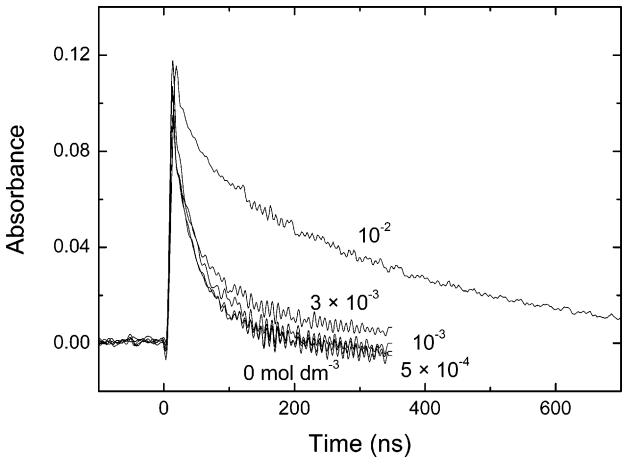

Figure 3. Absorption transient signals at 1000 nm of THF solutions containing different concentrations of $Sr(ClO_4)_2$.

For example, for an initial concentration of 10^{-2} mol dm^{-3} of salt $Ca(ClO_4)_2$ or $Sr(ClO_4)_2$ in THF, the concentration of ionic species for the calcium perchlorate is lower than 5×10^{-6} mol dm^{-3} and, for the strontium salt, lower than 2×10^{-6} mol dm^{-3}. This indicates clearly that the reactions between the solvated electron and perchlorates in THF must occur with the neutral form of the metallic salts, which are in huge excess compared to the ionic forms. Even if we admit an error in the estimation of the different limiting conductance used for the calculations, the results remain unchanged: the neutral forms of the salts are predominant in THF.

III.2. Kinetics of Pair Formation and Decay. In THF, the decay of the solvated electron, as observed in the infrared region, is very fast,[24] even in the absence of alkaline earth cations, and it lasts only a few tens of nanoseconds. It is worth noting that the mobility of the solvated electron in THF is very high.[25,26] The value of the rate constant of the recombination reaction 6 between solvated electrons and counter-radical cations in THF is diffusion controlled and larger than 10^{12} s^{-1} dm^{-3} mol^{-1} [27,28]

$$e_S^- + THF^+ \rightarrow \text{products} \qquad (6)$$

The nature of THF^+ is not known, and it stands for all radical cations produced by the pulse. Under our experimental conditions, even at lowest dose, the concentration of the solvated electron at the end of the pulse is quite high (around 5×10^{-6} mol dm^{-3}). To be able to compete with reaction 6, the concentration of a solvated electron scavenger should be chosen high enough. Therefore, we observed the kinetics in solutions containing different concentrations of $Ca(ClO_4)_2$ and $Sr(ClO_4^-)$ (pure solvent and 5×10^{-4} to 1×10^{-2} mol dm^{-3} in alkaline earth cation). The reaction occurring between the solvated electron and the cations Ca^{II} and Sr^{II} is faster than what we found with Mg^{II}.[8]

In Figure 2 the kinetics signals at 1000 nm are represented for solutions of $Ca(ClO_4)_2$ in THF for concentrations between 0 and 5×10^{-2} mol dm^{-3}. There are two kinds of kinetics: for the pure solvent and 10^{-3} mol dm^{-3}, the kinetics obey a second-order law, so at the concentration 10^{-3} mol dm^{-3} we observe only the solvated electron. For higher concentrations, we are in the presence of totally different kinetics, indicating that a new species is absorbing and that the formation reaction of this species is in competition with reaction 6. The apparent decay at 900 nm and after 20 ns is slowed relative to the decay observed in pure THF or below $\sim 10^{-4}$ mol dm^{-3}. This is supposed to be due to a pair (Ca^{II}, e_s^-) by analogy with the previous works on magnesium solutions in THF.[8] The formation of the pair is very fast and the decay seems to be a first-order process.

Figure 3 shows the absorption signals at 1000 nm obtained by irradiating solutions of $Sr(ClO_4)_2$ in THF with different concentrations of salt. We observe the same behavior as that for magnesium and calcium perchlorates. Similarly to the case of Ca^{II} solutions, below a threshold concentration, the absorption signals are similar to the signal of solvated electron, but above this threshold, a new kind of signal is appearing. This species is supposed to be the pair (Sr^{II}, e_s^-) and its absorption is clearly identifiable for a concentration of 10^{-2} mol dm^{-3}. The formation of this pair is also very rapid, as is its decay.

We assume here the validity of the mechanism we established previously for the magnesium solutions.[8] In addition to reaction 6 there is an equilibrium reaction between the solvated electron, M^{II} and the pair:

$$e_s^- + M^{II} \rightleftarrows (M^{II}, e_s^-) \qquad K_7 = \frac{[(M^{II}, e_s^-)]}{[M^{II}][e_s^-]} \qquad (7)$$

where M^{II} is either Ca^{II} or Sr^{II}. Moreover a spontaneous decay of the pair was assumed:

$$(M^{II}, e_S^-) \rightarrow P' \qquad (8)$$

To obtain the values of the rate constants and of the extinction coefficients of the pairs, we fitted the absorption signals by the probabilistic approach described previously (MCMC method). No identifiability problems were detected, in contrast with the study of Mg^{II}, where the rate of reaction 8 was too low and could not be identified. The estimated values and uncertainties of the parameters are reported in Table 1. The free enthalpy for equilibrium reaction 7, $\Delta G_7°$, is almost identical for the three pairs. In contrast, their lifetimes differ remarkably (decreasing in the series Mg^{II}, Ca^{II}, Sr^{II}) because of the increase of the value of k_8. In the previous work, we assigned reaction 8 to the internal reduction forming ClO_3^- according to

$$[M(ClO_4)_2(THF)_2, e^-] \rightarrow MO^+ClO_4^-ClO_3^-(THF)_2 \qquad (9)$$

We give the free enthalpy of this reaction for the three metals in Table 2. It can be seen that the calculated values are very negative, as already found for Mg in ref 8. Finally we note that the extinction coefficient of the pair $\epsilon(M^{II}, e_s^-)$ decreases along

TABLE 1: Estimations of the Parameters Resulting from the Probabilistic Analysis of the Transient Absorption with Reactions 6−8[a]

	Mg^{II}	Ca^{II}	Sr^{II}
k_7 (10^9 mol^{-1} dm^3 s^{-1})	6.2 ± 0.2	2.4 ± 0.3	4.5 ± 0.6
k_{-7} (10^6 s^{-1})	3.8 ± 0.1	3.5 ± 0.2	2.8 ± 0.2
k_8 (10^6 s^{-1})	<0.1	1.0 ± 0.2	2.2 ± 0.5
k_{11} (10^9 mol^{-1} dm^3 s^{-1})	7.0 ± 0.1	5.1 ± 0.1	9.5 ± 0.4
$\epsilon(e_s^-)$, M^{II}) (10^4 mol^{-1} dm^3 cm^{-1})	4.1 ± 0.1	3.3 ± 0.4	1.2 ± 0.1
K_7 (mol^{-1} dm^3)	1660 ± 50	686 ± 25	1607 ± 50
$\Delta G_7°$ (eV)	-0.19	-0.17	-0.19

[a] The values for Mg are reported from a previous study.[8] Other parameters have been fixed to their average values: $k_6 = 2 \times 10^{12}$ mol^{-1} dm^3 s^{-1}, $k_{10} = 3.9 \times 10^{10}$ mol^{-1} dm^3 s^{-1}, and $\epsilon(e_s^-) = 10^4$ mol^{-1} dm^3 cm^{-1}).

TABLE 2: Ab Initio Results for Total Free Enthalpies of Neutral and Anionic Perchlorates of Alkaline Earth in THF and Their Difference and the Free Enthalpy of Reactions 7 and 9

	G(neutral) (au)	G(anion) (au)	ΔG (eV)	$\Delta G_7°$[a] (eV)	$\Delta G_9°$ (eV)
Mg	−2186.611 947	−2186.654 553	−1.16	−0.26	−2.7
Ca	−2664.105 707	−2664.158 582	−1.44	− 0.54	−1.7
Sr	−2017.275 559	−2017.323 551	−1.31	−0.41	−1.9

[a] The solvation energy of electron in THF was assumed to be −0.9 eV.

the same series. The value is markedly low for the pair involving Sr^{II} (Table 1).

III.3. Reactivity of the (M^{II}, e_s^-) Pair with Biphenyl. The reaction between (M^{II}, e_s^-) and biphenyl is investigated over a biphenyl concentration range from 10^{-4} to 10^{-3} mol dm^{-3} in THF solutions containing 10^{-2} mol dm^{-3} of cation perchlorate. As examples, Figures 4 and 5 present the time profiles of the transient absorption signals monitored at 400 nm and 900 or 1000 nm upon pulse radiolysis of THF solution containing 10^{-2} mol dm^{-3} $M^{II}(ClO_4)_2$ and 5×10^{-4} mol dm^{-3} biphenyl. The signals at 400 nm show the appearance of the biphenylide radical anion, while the absorption signal at 900 or 1000 nm is mainly due to the (M^{II}, e_s^-) pair. Under the present experimental conditions, the pair is mostly formed within the electron pulse duration leading to a very fast rise in the absorbance in the infrared. Thereafter, the pair disappears following pseudo-first-order decay (inset of Figures 4 and 5).

We showed previously that the presence of $M^{II}(ClO_4)_2$ in solution significantly alters the shape of the signal at 400 nm.[19] In its absence, we observed a fast rise in the absorbance until 50 ns followed by a slow decay. In the presence of 10^{-2} mol dm^{-3} $M^{II}(ClO_4)_2$ the signal at 400 nm consists of three parts: first, a very fast increase within the electron pulse duration, due to the following reaction

$$Ph_2 + e_s^- \rightarrow Ph_2^- \qquad (10)$$

then, a supplementary rise in the absorbance reaching a maximum around 150 ns and, eventually, a slow decay lasting few hundreds of nanoseconds. The slow supplementary growth of the absorbance after the electron pulse, indicating a subsequent formation of Ph_2^-, is correlated to the decay of the pair at 900 or 1000 nm (Figures 4 and 5). We conclude that an electron transfer occurs from the (M^{II}, e_s^-) pair toward the biphenyl to produce the biphenylide ion according to reaction:

$$(M^{II}, e_s^-) + Ph_2 \rightarrow Ph_2^- + M^{II} \qquad (11)$$

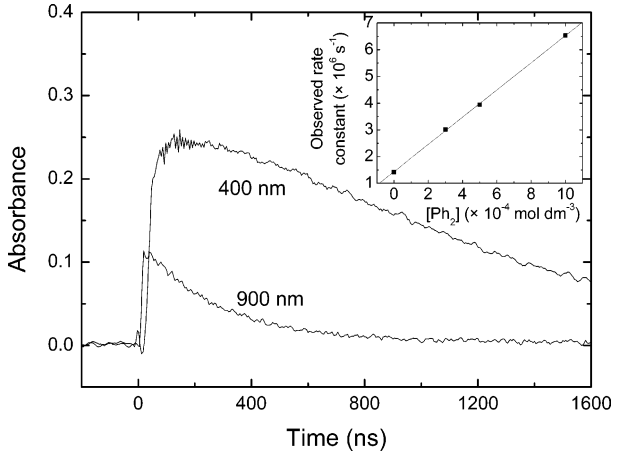

Figure 4. Time profile of the transient absorption signals monitored at 400 and 900 nm upon pulsed radiolysis of THF solution containing 10^{-2} mol dm^{-3} of calcium perchlorate and 3×10^{-4} mol dm^{-3} of biphenyl. Inset: First-order rate constant, k_{obs}, of the optical change observed at 900 nm.

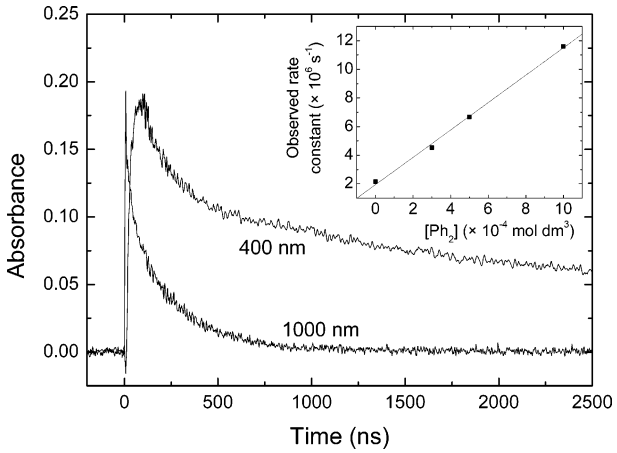

Figure 5. Time profile of the transient absorption signals monitored at 400 and 1000 nm upon pulsed radiolysis of THF solution containing 10^{-2} mol dm^{-3} of strontium perchlorate and 3×10^{-4} mol dm^{-3} of biphenyl. Inset: First-order rate constant, k_{obs}, of the optical change observed at 1000 nm.

We have evaluated k_{11} by probabilistic data analysis (Table 1) and also a pseudo-first-order analysis of the decay of the pairs as we reported in our previous paper. The estimated values are several times lower than that determined for the reduction of biphenyl by solvated electron ($k_9 = (3.9 \pm 0.1) \times 10^{10}$ dm^3 mol^{-1} s^{-1}). The pair involving Sr^{II} displays the highest reactivity in the series, followed by Mg^{II} and Ca^{II}.

III.4. Absorption Spectrum of the Pair. We first checked that for the solutions containing 10^{-2} M perchlorates of calcium and strontium the decays are wavelength independent. Therefore, the transient absorption spectra for solutions measured and reported in Figure 6 concern only one species, the product of reaction 7. They were measured 50 ns after the electron pulse. For comparison, we display in the same figure the spectrum previously obtained for the pair with magnesium. The absence of data around 1200 nm is due to the absorption of THF. The measured spectra are very wide and present two bands. The maxima are located at 980 and 1150 nm for (Mg^{II}, e_s^-), at 900 and 1070 nm for (Ca^{II}, e_s^-) and at 850 and 1050 nm for (Sr^{II}, e_s^-). For reference, the absorption spectrum of solvated electron is a single band located around 2250 nm.[24] The absorption band is increasingly shifted to the blue along the series (Mg^{II}, Ca^{II},

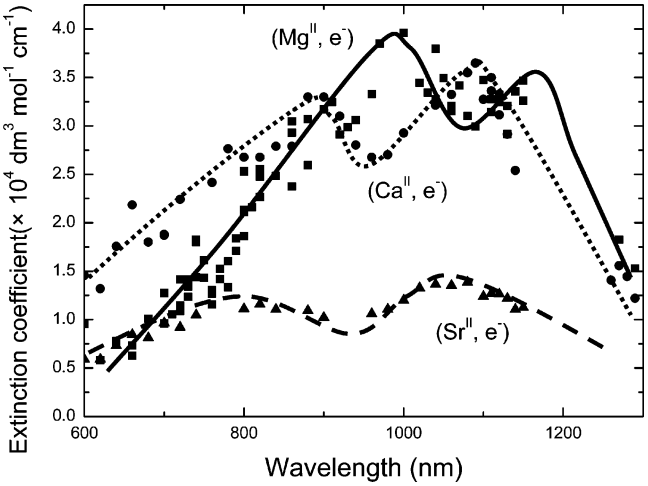

Figure 6. Transient absorption spectrum of the product of the reaction $M(ClO_4)_2 + e_s^-$ obtained by pulse radiolysis measurements recorded 50 ns after the pulse for a THF solution containing 10^{-2} mol L^{-1} M^{II}.

TABLE 3: Ab Initio Values of the Geometry Parameters of Neutral and Anion Forms of Alkaline Earth Perchlorates[a]

	distances and angles	Mg	Ca	Sr
neutral	*d*(MCl) (Å)	2.65	3.0	3.15
	ClMCl[b]	180	180	180
	OClClO[c]	90	90	90
anion	*d*(MCl) (Å)	2.9	3.15	3.31
	ClMCl[b]	104	107	109
	OClClO[c]	22	22	0

[a] M stands for metal cation (Mg^{II}, Ca^{II} and Sr^{II}). d(MCl) is the distance between the metal cation and the chlorine center of perchlorate. [b] Angle in degrees. [c] Dihedral angle in degrees: the two oxygens are the bottom oxygens of the structures of Figure 8.

Sr^{II}), in concert with an increase of the energy gap between the two peaks (ΔE (eV) = 0.18, 0.22, and 0.27, respectively).

III.5. Ab Intitio Description of the Pair Formation. The geometry parameters of the perchlorates of Mg^{II}, Ca^{II}, and Sr^{II} (neutral and anion forms) are given in Table 3. It can be seen that from Mg to Sr the metal−perchlorate distance increases, whatever the charge state. This can be easily related to the increasing size of the cation. It can be seen also that the pairing has dramatic consequences: metal−perchlorate distances increase, one perchlorate pivots (as the OClClO dihedral angle shows), and the system bends (as the ClMCl angle shows). For the anionic form, the value of the dihedral angle tends toward 0 from Mg to Sr. $Sr(ClO_4)_2^-$ is thus symmetrical, and presents C_{2v} symmetry, as can be seen in Figure 7.

In Figure 7 we show the shape of the SOMO (singly occupied molecular orbital) of the $[M(ClO_4)_2]^-$ pairs. These orbitals resemble each other, with a main lobe on the side of the solute. This shape is that of a diffuse sp hybrid of the metal and has also been found in $[Mg(H_2O)_n]^-$ gas-phase clusters.[29] In the case of Ca and Sr, an extension of the orbital between the perchlorates bears witness for the interference of the d states of Ca^+ and Sr^+. Actually, the first s → d transition energy in these ions (1.69 eV in Ca^+, 1.80 eV in Sr^+) is much lower than in Mg^+ (8.86 eV).[30] We have calculated the barycenter of the charge of these SOMO's to be 1.4 Å away from the metal cation.

Absolute values of the free enthalpies of the neutral perchlorates and of their anions are given in Table 2. From these values we can evaluate the free energy of the electron attachment:

$$M(ClO_4)_2(THF)_2 + e_s^- \rightarrow [M(ClO_4)_2(THF)_2]^- \quad (12)$$

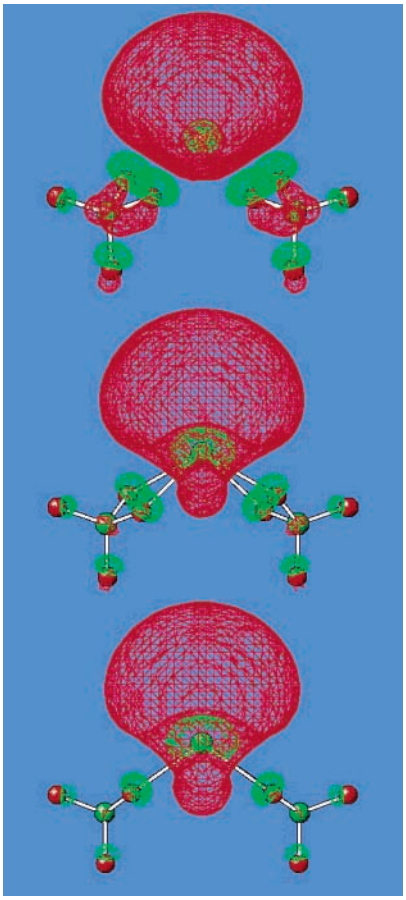

Figure 7. Optimized structures and isodensity surfaces of the SOMO (density value: 0.02 au) of the three solutes $Mg(ClO_4)_2$ (top), $Ca(ClO_4)_2$ (center), and $Sr(ClO_4)_2$ (bottom).

where the metal M stands for Mg, Ca, and Sr. This reaction is an explicit form of the forward reaction 7. The free enthalpy of this reaction (and of reaction 7) reads

$$\Delta G_7^\circ = G(\text{anion}) - G(\text{neutral}) - \Delta G_{sol}(e^-) \quad (13)$$

The last term of this equation has been evaluated in the first article[8] of this series to be −0.9 eV. In Table 2 we give the values of the free energies *G*(anion), *G*(neutral), and ΔG_7°. The values of ΔG_7° show that in every case reaction 7 is spontaneous, with free enthalpies −0.26 eV for Mg, −0.54 eV for Ca, and −0.41 eV for Sr. These numbers are consistent with the fact that the pair is observed but are overestimated (too negative), if compared to the values of Table 1. Nevertheless, we consider that the agreement is satisfactory, due to the difficulty of accurate calculations.

III.6. Effect of the Nature of Cations on the Absorption Spectrum of the Solvated Electron. From the theoretical simulation it is clear that the solvated electron cannot reduce the earth metal cations to monovalent cations in THF. Moreover, in THF several studies have shown that the solvated electron forms a pair with alkaline metal cations.[31] In water, at very high concentration of Li^+ and Na^+ (10 mol L^{-1}) a blue shift of the hydrated electron absorption spectra was also observed.[32] But the perturbed absorption spectra of hydrated electron in the presence of 10 mol L^{-1} of alkaline metal cations present only one large band with a maximum at 600 nm. The shift of the absorption band is attributed to an interaction with the metal cations changing the electron hydration energy.[33]

Despite many trials we could not obtain ab initio absorption spectra in satisfactory agreement with the measurements. The

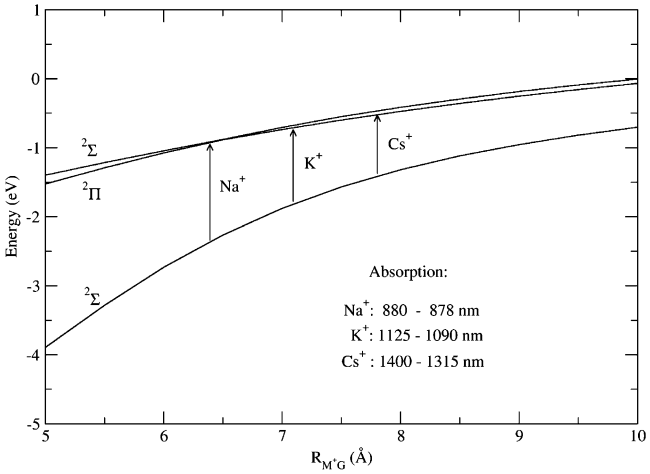

Figure 8. Diagram of potential energy curves of a solvated electron in interaction with an alkali cation in THF. G stands for the center of the Gaussian orbitals. The value of the two transitions for the same distance are given on the figure.

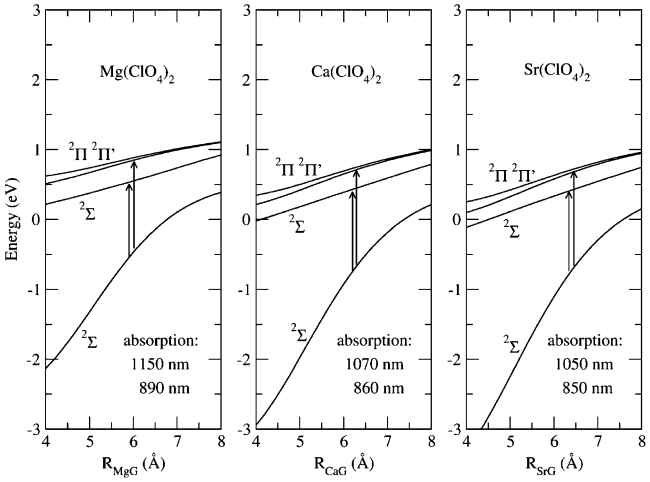

Figure 9. Potential energy curves of a solvated electron in interaction with the perchlorates of Mg, Ca, and Sr. G stands for the center of the Gaussian orbitals. The two arrows indicate the two transitions at the same distance.

calculated transition energies are generally too large, and oscillator strengths too small. We attribute this feature to ab initio calculations yielding too intimate pairs, of the "anion" type. This is consistent with the ab initio thermochemical results of Table 2, yielding pairs which are too stable. We now use the asymptotical method presented in section II.4.

III.6.1. Perturbation by Alkaline Cations. Our asymptotical model includes two physical effects: electrostatic interaction and polarization. These two effects yield diagonal and nondiagonal contributions, respectively, to the Hamiltonian matrix in the Gaussian orbitals basis set. The relative strengths of these two effects are ruled by the inequalities between nucleus attraction integrals:

$$\left\langle p_0, -\frac{1}{r_c} p_0 \right\rangle < \frac{1}{R} < \left\langle s, -\frac{1}{r_c} s \right\rangle < \left\langle p_{\pm 1}, -\frac{1}{r_c} p_{\pm 1} \right\rangle \ll \left\langle s, -\frac{1}{r_c} p_0 \right\rangle \quad (14)$$

where r_c is the distance of the electron to the cation nucleus and R the distance of the cation to the center of the Gaussians. The first terms of these inequalities rule the electrostatic interactions; the very last term rules the polarization in the Σ state. Of course polarization in the Π state, namely, $p_{\pm 1}/d_{\pm 1}$ orbital mixing, is also present. The potential energy curves are shown in Figure 8. The curves of the excited Σ and Π states cross each other at about 6.5 Å. This feature is due to the cancellation of electrostatic and polarization interactions: electrostatic contributions tend to split the excited states, with the Σ state more attractive than the Π state, according to eq 14; polarization tends to lower the first Π state because of the interaction with the second one (issued from the d type Gaussian orbital) not shown in Figure 8.

For each cation, the potential curves enable the finding of the experimental value of the transition energy. The corresponding cation/electron distances amount to 6.45, 7.1, and 7.8 Å, for Na^+, K^+, and Cs^+, respectively. These transitions are indicated by arrows in Figure 8. At these distances the two excited states, Σ and Π, are in principle observable, but the absorption wavelengths differ by 2 nm for Na^+ (due to the crossing), 35 nm for K^+, and 85 nm for Cs^+. Such differences cannot be distinguished in the IR broad absorption band. This result is consistent with recent molecular dynamics (MD) results, showing that the absorption spectrum of the solvated electron in aqueous solutions of Na^+ is a superposition of two neighboring bands.[5] These MD results actually show that the first absorption band corresponds to the $\Sigma \rightarrow \Pi$ transition. This feature is due to the core repulsion effect (see section II.4), which destabilizes the excited Σ state. Nevertheless, this effect is very small and not observable.

III.6.2. Perturbation by Alkaline Earth Perchlorates. We have first used the result of the conductimetry measurements and assumed that the perchlorates are nondissociated. The perchlorates have been modeled with the MK charges of the neutral species, at the optimized geometry of the anion. The corresponding potential energy curves for the three metals are shown in Figure 9. The three excited states are now nondegenerated, due to the complex geometry of the solutes. Since the degeneracy breaking of the Π states is actually weak, we note the states with Σ, Π, and Π' in Figure 9. The curves enable an interpretation of the spectrum: a metal−solute distance can be found, which yields the measured wavelength of the first band (with the largest wavelength). The wavelength of the second transition is taken at the same distance. These results are given in Table 4: it can be seen that the essential results, the wavelengths of the second absorption band, are in excellent agreement with the experimental values. The transition distances 5.9 (Mg), 6.2 (Ca), and 6.35 Å (Sr), are consistent with the increasing radii of their cations (see Table 4). Due to the MD results on Na^+ we must consider that core repulsion effects would also destabilize the excited Σ states of the alkaline earth systems. Nevertheless we note that alkaline earth dications are much smaller than the corresponding alkaline cations (see Table 4) and that they induce a much stronger degeneracy breaking. This tends to indicate that in the present case our asymptotic method is likely to yield the correct nature of the transitions.

To discuss these results, we have investigated several charge and geometry states of the magnesium perchlorate in THF: free Mg^{2+}, a result of complete dissociation of the salt; $MgClO_4^+$, a result of the partial dissociation; and nondissociated $Mg(ClO_4)_2$ with its D_{2d} equilibrium geometry (see Figure 8b of ref 8) and with the bent geometry of the anion (see Figure 7). All these species are possible solutes, if conductimetry measurements are ignored. Moreover, they display various charge distributions: Mg^{2+} has a charge +2, $MgClO_4^+$ has a charge +1 and a large dipole, and $Mg(ClO_4)_2$ (with D_{2d} symmetry) has no charge but presents a large quadrupole. In comparison, the bent $Mg(ClO_4)_2$ displays no charge but a large dipole. The potential energy

TABLE 4: Absorption Wavelengths for Alkali Cations and Alkaline Earth Perchlorates, Metal Charge, Solute Dipole Moments (D), Solute−Electron Distance R_{trans}, Ionic Radus R_{Ionic} of the Cations, and Solvent Distance R_{Solv} (See Equation 15) Obtained by the Asymptotic Model

	transition wavelengths (nm)							
	exptl	theor						
		$\Sigma \rightarrow \Sigma$	$\Sigma \rightarrow \Pi$	metal charge	dipole moment (D)	R_{trans} (Å)	R_{ionic} (Å)	R_{solv} (Å)
Na^+	880	880	878	+1.00	0.0	6.4	1.0	2.0
K^+	1125	1125	1090	+1.00	0.0	7.1	1.5	2.2
Cs^+	1400	1400	1315	+1.00	0.0	7.8	1.7	2.7
$Mg(ClO_4)_2$	1150−980	1150	900−880	+1.53	8.2	5.9	0.7	1.8
$Ca(ClO_4)_2$	1070−900	1070	870−850	+1.71	10.9	6.2	1.0	1.8
$Sr(ClO_4)_2$	1050−850	1050	865−840	+1.77	11.4	6.3	1.25	1.7

curves for these four species are shown in Figure 10. It can be seen that the curves are very different from each other. All these curves but one, that for $MgClO_4^+$, enable the identification of the transition distance, with two bands separated by roughly the right gap. Mg^{2+} yields a very large transition distance (9.5 Å). Since this distance is much larger than that obtained with the less charged Na^+ cation (6.4 Å), we conclude that Mg^{2+} cannot be the observed solute in THF. These two points are consistent with the experimental evidence that the perchlorates are nondissociated. Figure 10 shows that the potential curves are very sensitive to the geometry of $Mg(ClO_4)_2$. The gap between the two absorption bands (experimental: 170 nm) is clearly overestimated if the D_{2d} geometry is assumed (320 nm), but also, to a lesser extent, with the bent solute (260 nm). The right gap would very probably be obtained with bent solute with a smaller bending angle. Again, this is consistent with our general criticism of the ab initio results.

III.6.3. Unified Interpretation of the Spectrum of Solvated Electron When Paired with Alkali and Alkaline Earth Cations. Our results for alkali cations and alkaline earth perchlorates are summarized in Table 4. We recall that the solute−electron distance is an adjustable parameter, chosen so as to yield the measured value of the wavelength of the first absorption band.

The transition distances R_{trans} can be written as a sum of the ionic radius of the cation R_{ionic}, the radius of the electron cavity $R_{cav} = 3.4$ Å, and the "solvent distance" R_{solv}:

$$R_{trans} = R_{ionic} + R_{solv} + R_{cav} \qquad (15)$$

The values of these distances are given in Table 4. For all of the six solutes the (vacuum) transition distances are in the range of 6−8 Å. The corresponding solvent distances are more compact, in the range of 1.7−2.7 Å. These numbers refer to vacuum and must be decreased, so as to take the solvent dielectric constant into account. This suggests that there is no solvent between the solutes and the electron. This contact nature of the pairs has already been deduced from ESR data.[34] The degeneracy breaking is not visible in the case of alkali cations (largest band gap: 85 nm for Cs), because the transitions occur in the region of the Σ/Π crossing. This crossing is due to the polarization of the solvated electron by the charge of the cations, obeying a R^{-4} law as stated in section III.6.1.

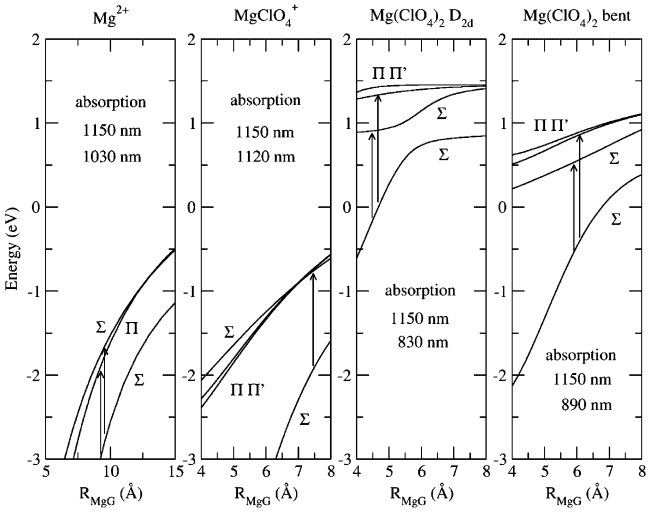

Figure 10. Potential energy curves of a solvated electron in interaction with different hypothetical solutes, coming from the dissociation of $Mg(ClO_4)_2$. G stands for the center of the Gaussian orbitals. The two arrows indicate the two transitions at the same distance.

By contrast, the degeneracy breaking is visible in the case of perchlorates. For understanding this feature we have used a simpler model of the solutes, actually a simple dipole. This procedure yielded results which are identical to those obtained with the complete set of MK charges (though at shorter solute electron distances). At long distance the degeneracy breaking is thus due to different electrostatic interactions in the excited states. This is ruled by inequalities, analogous to that of eq 14 for the alkali case. We note also than the degeneracy breaking is not canceled by polarization, unlike in the alkali case. This is due to the fact that neutral dipoles only weakly polarize the solvated electron, according to a R^{-6} law. We have checked that the polarization energies of the electron by a charge +1 and by the present neutral dipole are in the ratio 2000:1 at 5 Å.

The differential effect of the three alkalis is ruled by the increase of the transition distance, partly ruled by the increase of the ionic radius of the metal. The case of perchlorates is at first sight more subtle, because going from the lightest to the heaviest metal yields a blue shift of the absorption bands, unlike in the alkali case. Table 4 shows that passing from Mg to Sr actually yields an increase of the transition distance, like for the alkalis, but that the transition energies also increase. Table 4 shows that this effect is simply due to the increasing charges on the metals or in other words to the increasing dipoles of the solutes.

IV. Conclusions

In this series of article, we demonstrated that in THF the solvated electron reacts with the nondissociated alkaline earth perchlorate $M(ClO_4)_2$ and forms a pair (M^{II}, e_s^-). The structures of the pairs have been determined by ab initio calculations. The pairs present longer lifetimes than the solvated electron in THF. They are reducing agents which can even reduce biphenyl. The absorption spectra of the pairs are composed of two bands and can be interpreted as a perturbation of the solvated electron spectrum. We showed for the first time that the p-like excited state of the solvated electron can be split in the presence of molecules presenting a dipole. An asymptotic model yields a very useful tool for the analysis of the results. With its help we

could unify the results for dissociated alkali and nondissociated alkaline earth salts in THF: ionic solutes yield absorption spectra with only one absorption band; dipolar neutral solutes yield absorption spectra with two bands. In the case of perchlorates, the nondissociation of the salts observed by conductivity measurements is confirmed and the effect of charge distribution of the solute is identified. It is very interesting that the detailed structure of the solutes can be traced in the absorption spectrum of the pairs.

References and Notes

(1) Hart, E. J.; Boag, J. W. *J. Am. Chem. Soc.* **1962**, *84*, 1294.

(2) Gould, R. F., Ed. *Solvated Electron*; Advances in Chemistry Series 50; American Chemical Society: Washington, D.C., 1965.

(3) Migus, A.; Gauduel, Y.; Martin, J. L.; Antonetti, A. *Phys. Rev. Lett.* **1987**, *15*, 1559. Long, F. H.; Lu, H.; Eisenthal, K. B. *Phys. Rev. Lett.* **1990**, *64*, 1469. Gauduel, Y.; Pommeret, S.; Antonetti, A. *J. Phys. Chem.* **1993**, *97*, 134. Silvia, C.; Walhout, P. K.; Yokoyama, K.; Barbara, P. F. *Phys. Rev. Lett.* **1998**, *80*, 1086. Emde, M. F.; Baltuska, A.; Kummrow, A.; Pshenichinkov, M. S.; Wiersma, D. A. *Phys. Rev. Lett.* **1998**, *80*, 464. Assel, M.; Laenen, R.; Laubreau, A. *Chem. Phys. Lett.* **2000**, *317*, 13. Laenen, R.; Roth, T. *J. Mol. Struct.* **2001**, *598*, 37.

(4) Schnitker, J.; Rossky, P. J. *J. Chem. Phys.* **1987**, *86*, 3471. Rossky, P. J.; Schnitker, J. *J. Chem. Phys.* **1988**, *92*, 4277. Motakabbir, K. A.; Schnitker, J.; Rossky, P. J. *J. Chem. Phys.* **1989**, *90*, 691.

(5) Bratos, S.; Leicknam, J.-Cl. *Chem. Phys. Lett.* **1996**, *261*, 117. Bratos, S.; Leicknam, J.-Cl.; Borgis, D.; Staib, A. *Phys. Rev. E* **1997**, *55*, 7217. Nicolas, C.; Boutin, A.; Lévy, B.; Borgis, D. *J. Chem. Phys.* **2003**, *118*, 9689. Spezia R.; Nicolas, C.; Archirel, P.; Boutin, A. *J. Chem. Phys.*, in press.

(6) Buxton, G. V.; Greenstock, C. L.; Helman, W. P.; Ross, A. B. *J. Phys. Chem. Ref. Data* **1988**, 17. Buxton, G. V.; Mulazzani, Q. G.; Ross, A. B. *J. Phys. Chem. Ref. Data* **1995**, 24.

(7) Renou, F.; Mostafavi, M. *Chem. Phys. Lett.* **2001**, *335*, 363.

(8) Renou, F.; Mostafavi, M.; Archirel, P.; Bonazzola, L.; Pernot, P. *J. Phys. Chem. A* **2003**, *107*, 1506.

(9) Belloni, J.; Billiau, F.; Cordier, P.; Delaire, J.; Delcourt, M. O. *J. Phys. Chem.* **1978**, *82*, 532.

(10) Petzold, L. R. *Siam J. Sci. Stat. Comput.* **1983**, *4*, 136.

(11) Bonneau, R.; Wirz, J.; Zuberbühler, A. D. *Pure Appl. Chem.* **1997**, *69*, 979.

(12) Vajda, S.; Rabitz, H. *J. Phys. Chem.* **1988**, *92*, 701. Vajda, S.; Rabitz, H. *J. Phy. Chem.* **1994**, *98*, 5265.

(13) Walter, E.; Pronzato, L. *Identification of Parametric Models from Experimental Data*; Springer: New York, 1997.

(14) Beechem, J. M.; Ameloot, M.; Brand, L. *Chem. Phys. Lett.* **1985**, *120*, 466.

(15) Sivia, D. S. *Data Analysis: A Bayesian Tutorial*; Clarendon: Oxford, U.K., 1996.

(16) Gelman, A.; Carlin, J. B.; Stern, H. S.; Rubin, D. B. *Bayesian Data Analysis*; Chapman & Hall: London, 1995.

(17) Gilks, W. R.; Richardson, S.; Spiegelhalter, D. J. *Markov Chain Monte Carlo in Practice*; Chapman & Hall: London, 1996.

(18) Robert, C. P.; Casella, G. *Monte Carlo Statistical Methods*; Springer: New York, 1999.

(19) Renou, F.; Pernot, P.; Bonin, J.; Lampre, I.; Mostafavi, M. *J. Phys. Chem. A* **2003**, *107*, 6587.

(20) Frisch, M. J.; Trucks, G. W.; Schlegel, H. B.; Scuseria, G. E.; Robb, M. A.; Cheeseman, J. R.; Zakrzeweski, V. G.; Montgomery, J. A.; Stratmann, R. E.; Burant, J. C.; Dapprich, S.; Millam, J. M.; Daniels, A. D.; Kudin, K. N.; Strain, M. C.; Farkas, O.; Tomasi, J.; Barone, V.; Cossi, M.; Cammi, R.; Mennucci, B.; Pomelli, C.; Adamo, C.; Clifford, S.; Ochterski, J.; Petersson, G. A.; Ayala, P. Y.; Cui, Q.; Morokuma, K.; Malick, D, K.; Rabuck, A, D.; Raghavachari, K.; Foresman, J, B.; Ciolowski, J.; Ortiz, J. V.; Stefanov, B, B.; Liu, G.; Liashenko, A.; Piskorz, P.; Komaromi, I.; Gomperts, R.; Martin, R. L.; Fox, D. J.; Keith, T.; Al-Laham, M. A.; Peng, C. Y.; Nanayakkara, A.; Gonzalez, C.; Challacombe, M.; Gill, P. M. W.; Johnson, B. G.; Chen, W.; Wong, M. W.; Andres, J. L.; Head-Gordon, M.; Reploge, E. S.; Pople, J. A. *Gaussian 98*; Gaussian Inc.: Pittsburgh, PA, 1998.

(21) Muguet, F. F.; Gelabert, H.; Gauduel, Y. *J. Chim. Phys*. **1996**, *93*, 1808.

(22) Fuoss, R. M.; Kraus, C. A. *J. Am. Chem. Soc.* **1933**, *55*, 2387.

(23) De Groof, B.; De Smedt, C.; Vankerckhoven, H.; Van Beylen, M. *Bull. Soc. Chim. Belg.* **1990**, *99*, 1065.

(24) Dorfman, L. M.; Jou, F. Y.; Wageman, R. *Ber. Bunsen-Ges. Phys. Chem.* **1971**, *75*, 681.

(25) Dodelet, J. P.; Freeman, G. R. *Can. J. Chem.* **1975**, *53*, 1263.

(26) Delaire, J.; Delcourt, M. O.; Belloni, J. *J. Phys. Chem.* **1980**, *84*, 1186.

(27) Cipollini, N. E.; Holroyd, R. A.; Nishikawa, M. *J. Chem. Phys.* **1977**, *67*, 4636.

(28) Jou, F. Y.; Dorfman, L. M. *J. Chem. Phys.* **1973**, *58*, 4715.

(29) Reinhard, B. M.; Niedner-Schatteburg, G. *J. Chem. Phys.* **2003**, *118*, 3571.

(30) Moore, C. E. *Natl. Bur. Stand. Circ. (U.S.)* **1949**, *467*.

(31) Fisher, M.; Ramme, G.; Claesson, S.; Szwarc, M. *Chem. Phys. Lett.* **1971**, *9*, 309.

(32) Gauduel, Y.; Pommeret, S.; Antonetti, A. *J. Phys. IV* **1991**, *1*(C5), 127.

(33) Impey, R. W.; Madden, P. A.; McDonald, I. R. *J. Chem. Phys.* **1983**, *87*, 5071.

(34) Seddon, W. A.; Fletcher, J. W.; Catterall, R. *Can. J. Chem.* **1977**, *55*, 2017.